Check for updates

New Phytologist

Research

Synthetically induced *Arabidopsis thaliana* autotetraploids provide insights into the analysis of meiotic mutants with altered crossover frequency

Pablo Parra-Nunez[1], Nadia Fernández-Jiménez[2], Miguel Pachon-Penalba[3], Eugenio Sanchez-Moran[1], Mónica Pradillo[2]* and Juan Luis Santos[2]*

[1]School of Biosciences, University of Birmingham, Edgbaston, Birmingham, B15 2TT, UK; [2]Departamento de Genética, Fisiología y Microbiología, Facultad de Ciencias Biológicas, Madrid, 28040, Spain; [3]Wellcome Centre for Cell Biology, Institute of Cell Biology, University of Edinburgh, Michael Swann Building, Max Born Crescent, Edinburgh, EH9 3BF, UK

Author for correspondence:
Mónica Pradillo
Email: pradillo@bio.ucm.es

Received: *2 March 2023*
Accepted: *29 September 2023*

New Phytologist (2023)
doi: 10.1111/nph.19366

Key words: Arabidopsis, autopolyploid, chiasma, colchicine, crossover, homologous recombination, meiosis, polyploid.

Summary

- Mutations affecting crossover (CO) frequency and distribution lead to the presence of univalents during meiosis, giving rise to aneuploid gametes and sterility. These mutations may have a different effect after chromosome doubling. The combination of altered ploidy and mutations could be potentially useful to gain new insights into the mechanisms and regulation of meiotic recombination; however, studies using autopolyploid meiotic mutants are scarce.
- Here, we have analyzed the cytogenetic consequences in colchicine-induced autotetraploids (colchiploids) from different Arabidopsis mutants with an altered CO frequency.
- We have found that there are three types of mutants: mutants in which chiasma frequency is doubled after chromosome duplication (*zip4*, *mus81*), as in the control; mutants in which polyploidy leads to a higher-than-expected increase in chiasma frequency (*asy1*, *mer3*, *hei10*, and *mlh3*); and mutants in which the rise in chiasma frequency produced by the presence of two extrachromosomal sets is less than doubled (*msh5*, *fancm*). In addition, the proportion of class I/class II COs varies after chromosome duplication in the control.
- The results obtained reveal the potential of colchiploid meiotic mutants for better understanding of the function of key proteins during plant meiosis. This is especially relevant considering that most crops are polyploids.

Introduction

Meiosis is a highly conserved and specialized cell division in eukaryotes, and it is essential for sexual reproduction. It is a two-step division process that takes place in the germ line and halves the number of chromosomes from a diploid cell, leading to the formation of haploid gametes. During the first meiotic division, homologous recombination is required to pair the homologous chromosomes into bivalents and to ensure regular chromosome segregation. Linkage between homologous chromosomes is maintained until anaphase I by reciprocal crossovers (COs), cytologically defined as chiasmata, and sister chromatid cohesion. Crossovers result in new combinations of alleles in the gametes, ensuring genomic variability in the offspring.

Factors controlling meiotic recombination in plants have been extensively studied over the last decades, particularly in the model species *Arabidopsis thaliana* (see the reviews Osman *et al.*, 2011; Mercier *et al.*, 2015; Wang & Copenhaver, 2018; Gutiérrez Pinzón *et al.*, 2021). Proteins involved in either double-strand break (DSB) formation or processing and elements of the chromosomal axes are essential to ensure the formation of COs, which may be generated from at least two coexisting pathways (class I and class II) controlled by different genes. Class I COs are subject to positive interference and, therefore, nonrandomly distributed, whereas class II COs are noninterfering. The percentage of COs attributed to each class differs among species, but in most organisms, the main meiotic CO pathway generates class I COs (Baker *et al.*, 1996; Copenhaver *et al.*, 2002; de los Santos *et al.*, 2003). In *A. thaliana*, class I COs represent *c.* 85% of all COs (Berchowitz *et al.*, 2007; Higgins *et al.*, 2008a). In this species, a wide number of proteins directly related to the control and formation of these two CO pathways have already been described (Mercier *et al.*, 2015). Among these proteins, MSH4 and MSH5, related to the prokaryotic MutS proteins (Higgins *et al.*, 2004, 2008b), seem to play an important role in the stabilization of double Holliday junctions (dHjs) and are grouped in a heterogeneous group of proteins called ZMM. Besides MSH4 and MSH5, this group is also composed of proteins that could play a regulatory role, such as the tetratricopeptide repeat protein ZIP4, the helicase MER3, or the ubiquitin E3 ligase HEI10 (Chen *et al.*, 2005; Mercier *et al.*, 2005; Chelysheva *et al.*, 2007, 2012). Interestingly, the cellular abundance of the latter controls the

*Joint senior authorship.

© 2023 The Authors
New Phytologist © 2023 New Phytologist Foundation
This is an open access article under the terms of the Creative Commons Attribution-NonCommercial-NoDerivs License, which permits use and distribution in any medium, provided the original work is properly cited, the use is non-commercial and no modifications or adaptations are made.

intensity of CO interference (Morgan *et al.*, 2021). In addition, two proteins have been reported to have a major function resolving the dHjs to form interference-sensitive COs, MLH1, and MLH3, which are homologs of the prokaryotic MutL (Franklin *et al.*, 2006). Regarding noninterfering COs, MUS81 and FANCD2 have been reported to influence the level of this type of exchanges in *A. thaliana* (Berchowitz *et al.*, 2007; Kurzbauer *et al.*, 2018). Moreover, there are anti-recombination mechanisms, affecting class II COs regulated from different pathways depending on: FANCM and its cofactors MHF1 and MHF2 (Crismani *et al.*, 2012; Knoll *et al.*, 2012; Girard *et al.*, 2014); members of the BLM-TOP3-RMI1 (BTR) complex (Séguéla-Arnaud *et al.*, 2015, 2017); and FIGL1 and its interacting protein FLIP1 (Girard *et al.*, 2015; Fernandes *et al.*, 2018). To add further complexity to this landscape, FANCD2, FANCM, RMI1, and FIGL1 contribute to normal distribution of class I CO to maintain CO assurance (Li *et al.*, 2021). Another group of proteins required to ensure proper CO formation consists of components of the proteinaceous axes that organize the chromosomes during meiosis. In *A. thaliana*, mutants deficient in either ASY1, ASY3, or ASY4 show disrupted axis organization and a substantial reduction in chiasmata (Ross *et al.*, 1997; Sanchez-Moran *et al.*, 2001; Armstrong *et al.*, 2002; Ferdous *et al.*, 2012; Chambon *et al.*, 2018).

Mutations affecting CO formation lead to the presence of univalents during meiosis I, giving rise to aneuploid gametes. Nevertheless, these mutations may have a different effect when more than two potential partners to pair and recombine with are available, that is in a polyploid context. Meiotic studies conducted with autopolyploid meiotic mutants are scarce, despite they can offer important new insights into the meiotic recombination mechanisms (Tian *et al.*, 2011; Roelens *et al.*, 2015). This may be due to the technical limitation of generating polyploid individuals in most species. In *A. thaliana*, the conversion of diploid into autotetraploid plants by using colchicine is relatively easy (Santos *et al.*, 2003; Yu *et al.*, 2009; Pecinka *et al.*, 2011; Parra-Nunez *et al.*, 2020).

In this study, we have analyzed the consequences of chromosome doubling by colchicine in different *A. thaliana* mutants with an altered CO frequency but no chromosomal fragmentation defects. We want to address whether the presence of more homologous chromosomes in the mutants increases the chances of finding homologous sequences to recombine in a homologous recombination-limited situation. For this purpose, eight different meiotic mutants have been selected: (1) *asy1* (defective for an axis-associated protein required for synapsis and CO formation); (2) *zip4*, *msh5*, *mer3*, and *hei10* (ZMM mutants that are proficient for synapsis but only have class II COs); (3) *mlh3* (in which the endonuclease activity critical for the formation of class I COs is missing), and *mus81* (defective for an structure-specific endonuclease required for class II CO formation); (4) *fancm* (hyper-recombinant mutant with an increased frequency of class II COs). All these mutants have been previously described at the cytological level during meiosis (Mercier *et al.*, 2005; Jackson *et al.*, 2006; Chelysheva *et al.*, 2007, 2012; Sanchez-Moran *et al.*, 2007; Higgins *et al.*, 2008a,b; Knoll *et al.*, 2012). Here, we have extended the study of these mutants in a polyploid context, in order to compare the response of the different mutants with respect to the chiasma frequency and chromosome configurations at metaphase I.

Materials and Methods

Plant material and growing conditions

The following *Arabidopsis thaliana* (L.) Heynh T-DNA insertion lines were used to produce mutant autopolyploid lines: *asy1-1* (SALK_144182), *zip4-2* (SALK_068052), *msh5-1* (SALK_110240), *mer3-1* (SALK_045941), *hei10-2* (SALK_014624), *mlh3-1* (SALK_015849), *mus81-2* (SALK_107515), and *fancm-1* (SALK_069784). The accession Columbia (Col-0) was used as the wild-type (WT) reference. The lines were obtained from the T-DNA mutant collection at the Salk Institute Genomics Analysis Laboratory via Nottingham Arabidopsis Stock Centre (NASC, Nottingham, UK). The primer sequences used for genotyping are listed in Supporting Information Table S1.

Seeds were sown on a sterilized mix of soil (75%) and vermiculite (25%) and grown under controlled environmental conditions: 16 h : 8 h, light : night photoperiod, 19°C temperature, and 60% relative humidity. After checking the genotype, the synthetic autopolyploids were generated according to the one-drop method described in Yu *et al.* (2009) and Parra-Nunez *et al.* (2020), applying a drop (10 µl) of colchicine (0.25% w/v) at the center of the plant rosette, before the first flowering. The chromosome number ($2n = 20$) of the surviving plants (*c.* 10–20%) was verified by cytological analyses. Aneuploid plants were discarded for the analyses. Due to the meiotic instability caused by chromosome doubling, the cytogenetic study was conducted in the same generation in which colchicine was applied, using three plants per genotype.

Cytogenetic analyses

Immature flower buds were fixed in Carnoy (6 ethanol : 3 chloroform : 1 acetic acid) and stored in fixative until required. The spreading technique was conducted following the procedure previously described by Fransz *et al.* (1998), with modifications included in Parra-Nunez *et al.* (2020) in order to obtain high-quality spreads of metaphase I chromosomes in which the chromosomal configurations can be differentiated.

The fluorescence *in situ* hybridization (FISH) technique was performed following the protocol described by Sanchez-Moran *et al.* (2001), with minor changes described in Parra-Nunez *et al.* (2020). The following rDNA probes were used: 5S rDNA from *A. thaliana* cloned in the pCT4.2 plasmid (Campell *et al.*, 1992), and 45S rDNA from *Triticum aestivum* cloned in the pTa71 plasmid (Gerlach & Bedbrook, 1979). The probes were labeled with modified dUTPs conjugated with Cy3 (Merck, Darmstadt, Germany) or FITC (Agrisera, Vännäs, Sweden) by nick-translation. Slides were mounted in 10 µl DAPI (1 µg ml^{-1}) in Vectashield mounting medium (Vector Laboratories, Newark, CA, USA) and imaged using an Olympus BX61 epifluorescence microscope equipped with a digital camera CCD (Olympus DP71; Evident Corporation, Tokyo, Japan).

© 2023 The Authors
New Phytologist © 2023 New Phytologist Foundation

14698137, 0, Downloaded from https://nph.onlinelibrary.wiley.com/doi/10.1111/nph.19366 by LEIBNIZ-INST. OF PLANT GENETICS AND CROP PLANT, Wiley Online Library on [23/11/2023]. See the Terms and Conditions (https://onlinelibrary.wiley.com/terms-and-conditions) on Wiley Online Library for rules of use; OA articles are governed by the applicable Creative Commons License

14698137, 0, Downloaded from https://nph.onlinelibrary.wiley.com/doi/10.1111/nph.19366 by LEIBNIZ-INST. OF PLANT GENETICS AND CROP PLANT, Wiley Online Library on [23/11/2023]. See the Terms and Conditions (https://onlinelibrary.wiley.com/terms-and-conditions) on Wiley Online Library for rules of use; OA articles are governed by the applicable Creative Commons License

Metaphase I images from each genotype were scored for the frequency of chiasmata as well as for the chromosomal configurations. At least two plants of each genotype were analyzed. The criteria used are described in Sybenga (1975), Sanchez-Moran *et al.* (2001), Santos *et al.* (2003), and Parra-Nunez *et al.* (2020).

For immunostaining of pachytene spreads, we conducted the protocol described by Sanchez-Moran *et al.* (2007) and Armstrong *et al.* (2009), with minor modifications. The following primary antibodies were used: α-MLH1 (rabbit, 1 : 500, Jackson *et al.*, 2006), α-HEI10 (rabbit, 1 : 500, Lambing *et al.*, 2015), and α-ZYP1 (rat, 1 : 1000, Higgins *et al.*, 2005). Closed flower buds from at least three different plants were used. The following secondary antibodies were used at 1 : 500 dilutions: α-rabbit-Alexa Fluor 555 (Agrisera), and α-rat-Alexa Fluor 488 (Agrisera). Individual cell images were acquired as Z-stacks (Olympus BX61, DP71), and the maximum intensity projection for each cell was rendered using ImageJ (Z project). Image deconvolution was implemented using the iterative algorithm Richardson-Lucy (DeconvolutionLab2, ImageJ plugin). We scored all images blind to genotype.

RNA extraction and reverse transcription-quantitative PCR

Total RNA was obtained from both 10-d seedlings (*c.* 50 seedlings per sample) and immature flower buds (from at least 10 different plants per sample) using the commercial kit InviTrap® Spin Plant RNA Mini Kit (Invitrogen) according to the manufacturer's instructions. Reverse transcription-quantitative PCR (RT-qPCR) was performed using the LightCycler®480 system (Hsieh *et al.*, 2016) in the facilities provided by 'Parque Científico de Madrid' (Universidad Autónoma de Madrid, Madrid, Spain). The probes applied belong to the Universal Probe Library (UPL, Roche). The genes assessed, primers, and UPL probes used are listed in Table S2. Three technical replicates of one or two independent RNA extractions obtained from different biological samples were performed, and two reference genes were used for data normalization: *ACTIN2* and *YLS8*. These reference genes were selected due to their adequacy in analyses involving diploid and tetraploid individuals according to the data published by Wang *et al.* (2014). The data were analyzed using the double delta C_t method (Livak & Schmittgen, 2001). To calculate the ΔC_t, the mean C_t value was normalized using the average of the mean C_t values obtained for both reference genes (average of mean $C_{t\ ACTIN2}$ and mean $C_{t\ YLS8}$; Riedel *et al.*, 2014).

Results

Chromosome identification and chiasma frequency analysis in autotetraploid crossover-deficient mutants

Although the mean cell chiasma frequencies of CO-deficient mutants selected for this study had been previously determined (Sanchez-Moran *et al.*, 2001; Mercier *et al.*, 2005; Jackson *et al.*, 2006; Chelysheva *et al.*, 2007, 2012; Higgins *et al.*, 2008a, b; Knoll *et al.*, 2012), we analyzed their values under our laboratory conditions and using FISH to improve the interpretation of the chiasmata present in the observed bivalents (Figs S1, S2). Moreover, a simultaneous comparison of these mutants with each other has not been carried out so far. It is important to note that chiasma scoring is a valuable, direct, and rapid approach to quantify reciprocal recombination at a genome-wide level in a polyploid context (Santos *et al.*, 2003; Higgins *et al.*, 2014; Bomblies *et al.*, 2016; Parra-Nunez *et al.*, 2019, 2020). Indeed, alternative methodologies based on the use of reporter lines and either pollen tetrad or seed analysis are not feasible here because the neotetraploids were analyzed in the same generation in which colchicine was applied and they did not produce tetrads but polyads.

Due to the existence of differences among all genotypes regarding mean cell chiasma frequency (Welch's ANOVA, $W(8.0, 212.5) = 831.6.1$, $P < 0.001$), pairwise comparisons using the Dunnett's T3 *post hoc* test were made. As expected, *asy1* 2× (2.10 ± 0.13, $n = 101$, $P < 0.001$), *zip4* 2× (1.65 ± 0.08, $n = 255$, $P < 0.001$), *msh5* 2× (1.77 ± 0.14, $n = 57$, $P < 0.001$), *mer3* 2× (3.36 ± 0.22, $n = 36$, $P < 0.001$), *hei10* 2× (2.07 ± 0.24, $n = 29$, $P < 0.001$), and *mlh3* 2× (4.18 ± 0.19, $n = 91$, $P < 0.001$) presented a significant decrease in CO formation respect to the WT (10.20 ± 0.14, $n = 70$, Figs S1, S2). On the contrary, neither *mus81* 2× (10.31 ± 0.12, $n = 101$, $P > 0.999$) nor *fancm* 2× (10.49 ± 0.23, $n = 67$, $P = 0.918$) showed differences compared with the WT (Figs S1, S2). It is worth mentioning that the corresponding mutant alleles had already been characterized as showing apparently normal meiosis and near WT chiasma frequency (Higgins *et al.*, 2008a; Knoll *et al.*, 2012). We also conducted a comparison of the mean cell chiasma frequency among the *zmm* mutants ($F(3.0, 373.0) = 20.49$, $P < 0.001$), since all of them are defective for the same type of COs (class I) and, in principle, they should only maintain class II COs. *mer3* 2× displayed a mean cell chiasma frequency significantly higher than those observed in *zip4* 2× ($P < 0.001$ vs *mer3* 2×), *msh5* 2× ($P < 0.001$ vs *mer3* 2×), and *hei10* 2× ($P = 0.001$ vs *mer3* 2×). On the contrary, we did not detect any differences among the latter ($P = 0.505$, *zip4* 2× vs *msh5* 2×; $P = 0.235$, *zip4* 2× vs *hei10* 2×; $P = 0.500$, *msh5* 2× vs *hei10* 2×; Table S3).

We also performed chiasma frequency analyses on colchiploids ($W(8.0, 193.9) = 1272$, $P < 0.001$). In this case, we not only observed univalents and bivalents at metaphase I, but also multivalents (Fig. 1). Like in diploids, the application of FISH significantly helped in the interpretation of chromosomal configurations and in the estimation of the number of chiasmata at metaphase I (Sanchez-Moran *et al.*, 2001; Parra-Nunez *et al.*, 2019, 2020). Differences in chiasma frequency with respect to the control (19.99 ± 0.11, $n = 186$) were again detected in all those mutants that had already shown a different behavior respect to the WT in the diploid condition (Dunnett's T3 *post hoc* test): *asy1* 4× (6.02 ± 0.32, $n = 54$, $P < 0.001$), *zip4* 4× (3.85 ± 0.43, $n = 26$, $P < 0.001$), *msh5* 4× (2.58 ± 0.17, $n = 113$, $P < 0.001$), *mer3* 4× (8.31 ± 0.56, $n = 42$, $P < 0.001$), *hei10* 4× (6.92 ± 0.37, $n = 61$, $P < 0.001$), and *mlh3* 4× (9.57 ± 0.32, $n = 61$, $P < 0.001$; Fig. 2a). Interestingly, *fancm* 4× (18.54 ± 0.21, $n = 96$, $P < 0.001$) showed a significantly lower chiasma frequency than the WT, unlike what happens in diploid condition.

© 2023 The Authors
New Phytologist © 2023 New Phytologist Foundation

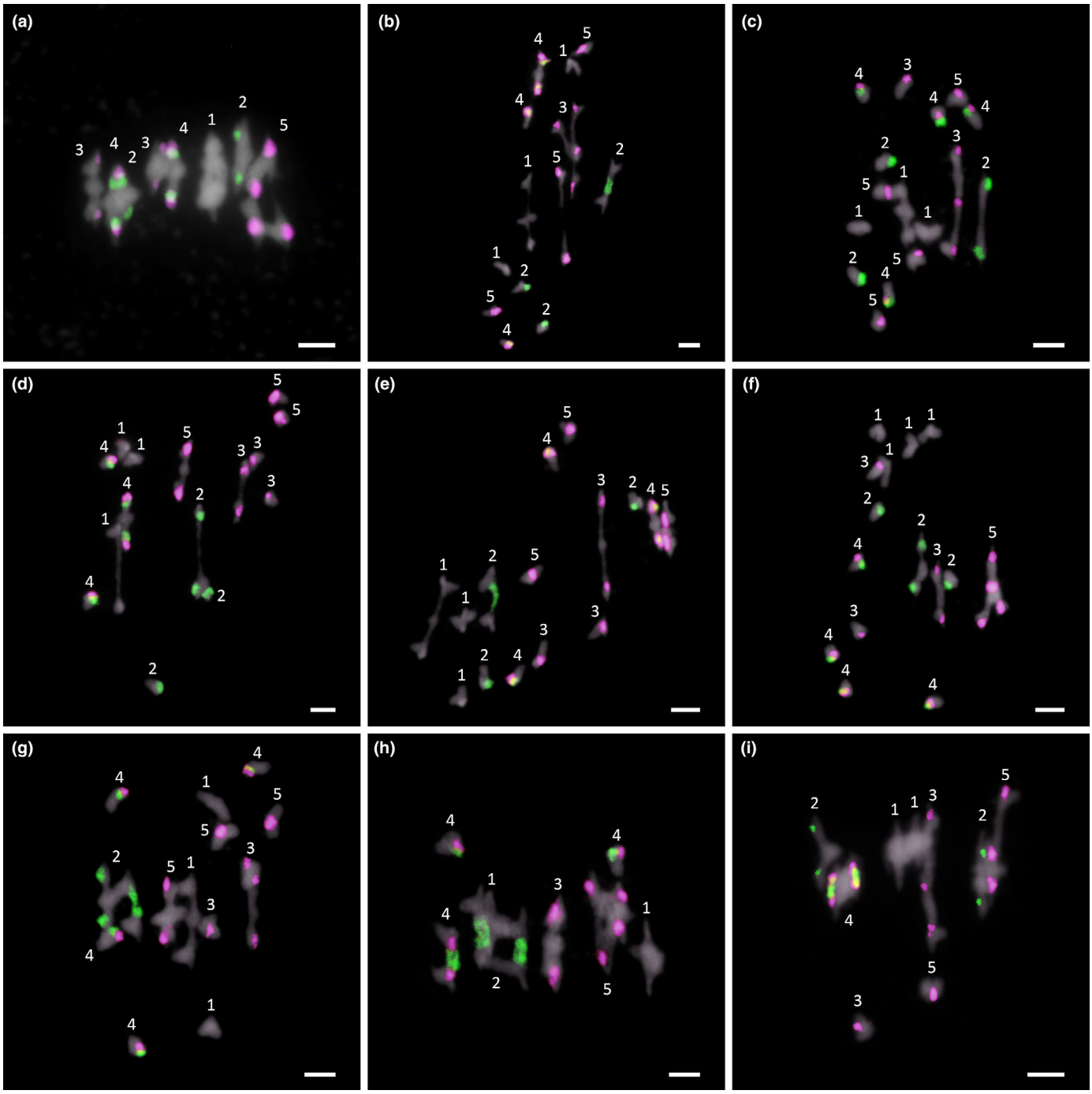

Fig. 1 Cytological analysis of *Arabidopsis thaliana* male meiocytes at metaphase I in colchiploid mutants with altered crossover frequency. Representative examples of metaphases I from Columbia (Col-0) 4× and the tetraploid mutants. (a) Col-0 4×: chromosomes 2, 3, and 4 are associated as II, whereas chromosomes 1 and 5 are forming IV; (b) *asy1* 4×: all groups of four homologous chromosomes appear as II + 2 I, except for chromosomes 3 that are associated forming a IV; (c) *zip4* 4×: chromosomes 4 and 5 appear as I, whereas chromosomes 1, 2, and 3 are present as II + 2 I; (d) *msh5* 4×: all groups of four homologous chromosomes appear as II + 2 I; (e) *mer3* 4×: all groups of four homologous chromosomes appear as II + 2 I; (f) *hei10* 4×: chromosomes 1 and 4 appear as I, chromosomes 2 and 3 as II + 2 I, and chromosomes 5 are associated forming a IV; (g) *mlh3* 4×: chromosomes 1 and 5 are forming II + 2 I, chromosomes 2 are associated as a IV, chromosomes 3 appear as III + I, and all chromosomes 4 appear as I; (h) *mus81* 4×: chromosomes 2, 3, and 5 are associated as IV, chromosomes 1 as II, and chromosomes 4 as II + 2 I; (i) *fancm* 4×: chromosomes 1 and 2 are associated as II, chromosomes 3 and 5 appear as III + I, and chromosomes 4 are forming a IV. Chromosomes were identified by fluorescence *in situ* hybridization (FISH) using 5S (magenta) and 45S rDNA (green) probes. Bars, 5 μm.

On the contrary, *mus81* 4× (19.52 ± 0.22, $n = 66$, $P = 0.343$) was the only mutant that did not display differences with respect to the tetraploid control. The *zmm* tetraploid mutants (*zip4* 4×, *msh5* 4×, *mer3* 4×, and *hei10* 4×) were also different from each other ($W(3.0, 75.30) = 61.16$, $P < 0.001$). As well as in diploid condition, *zip4* 4× and *msh5* 4× presented similar mean cell

© 2023 The Authors
New Phytologist © 2023 New Phytologist Foundation

14698137, 0, Downloaded from https://nph.onlinelibrary.wiley.com/doi/10.1111/nph.19366 by LEIBNIZ-INST. OF PLANT GENETICS AND CROP PLANT, Wiley Online Library on [23/11/2023]. See the Terms and Conditions (https://onlinelibrary.wiley.com/terms-and-conditions) on Wiley Online Library for rules of use; OA articles are governed by the applicable Creative Commons License

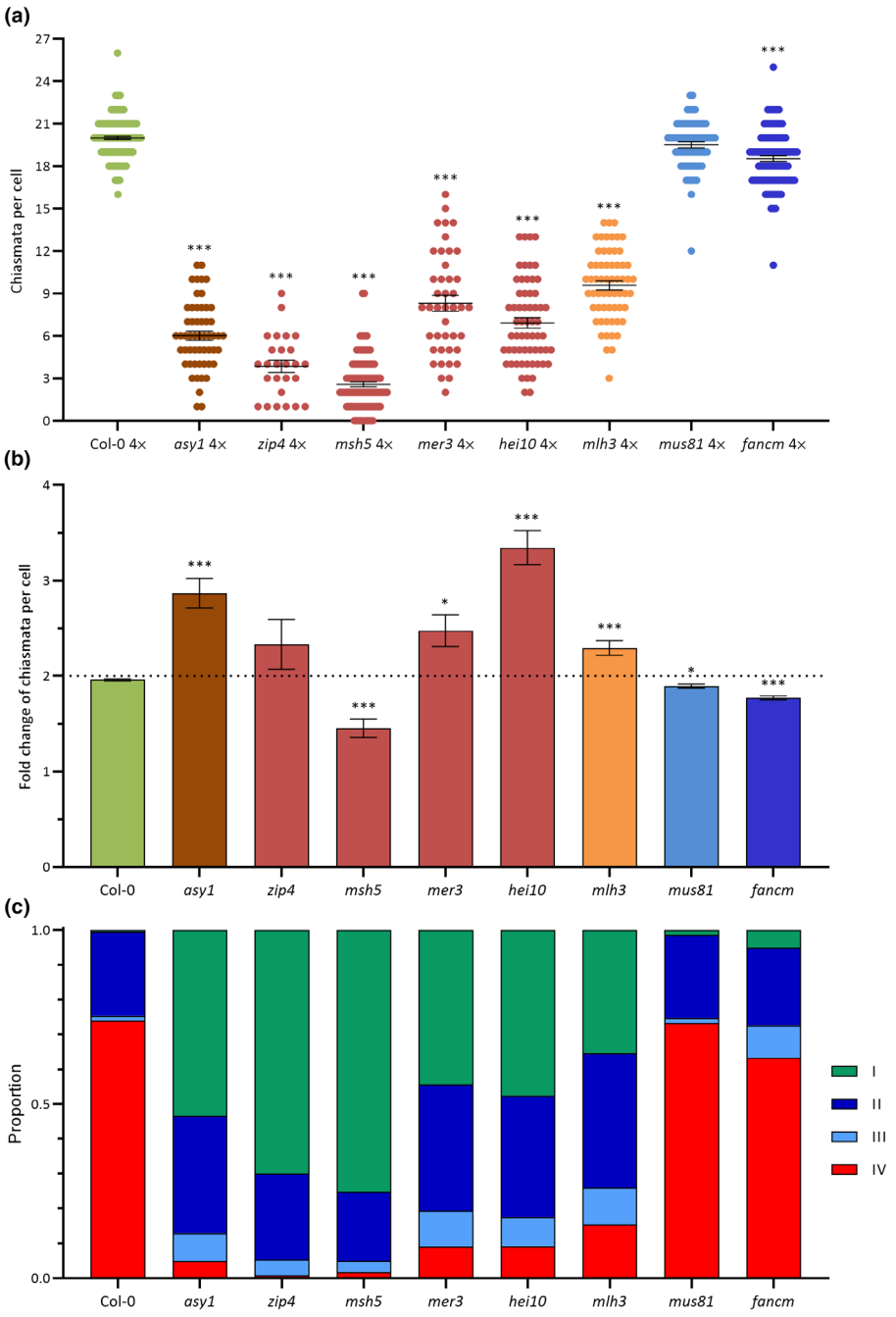

Fig. 2 Analysis of chiasma frequency and chromosome configurations at metaphase I in *Arabidopsis thaliana* colchiploid mutants with altered crossover frequency. (a) Scatter plots representing the total mean chiasma frequency per cell corresponding to the different mutants analyzed. Error bars represent the SE of the mean. Statistical comparison with the control is shown for those mutants in which differences were detected (Dunnett's T3 *post hoc* test; ***, $P < 0.001$). (b) Fold change between the corresponding tetraploid and diploid chiasma frequencies per cell. Error bars represent the SE of the mean. Statistical comparison with the control is shown for those mutants in which differences were detected (Dunnett's T3 *post hoc* test; *, $P < 0.05$; ***, $P < 0.001$). (c) Proportion of the different chromosomal configurations (I, univalents; II, bivalents; III, trivalents; IV, quadrivalents) per meiocyte at metaphase I.

chiasma frequencies ($P = 0.057$). However, *hei10* 4× showed a different behavior with respect to *hei10* 2×: no difference from *mer3* 4× ($P = 0.223$), and a higher chiasma frequency than *zip4* 4× and *msh5* 4× ($P < 0.001$ in both cases; Table S3). Despite the change in chiasma frequency in *hei10* 4× with respect to the other *zmm* mutants, distribution of chiasmata between cells fitted a Poisson distribution (Kolmogorov–Smirnov test, $D = 0.242$, $P = 0.287$), just as in *hei10* 2× ($P = 0.878$; Fig. S3).

To understand the change in chiasma frequency after genomic duplication, the fold change between the corresponding tetraploid and diploid chiasma frequencies (4×/2×) was calculated (Fig. 2b). Overall chiasma frequency was approximately doubled in the WT (1.96 ± 0.01). *Post hoc* pairwise comparisons showed that *asy1* (2.87 ± 0.15, $P < 0.001$), *mer3* (2.47 ± 0.17, $P < 0.05$), *hei10* (3.34 ± 0.18, $P < 0.001$), and *mlh3* (2.29 ± 0.08, $P < 0.001$) had a significantly higher fold change than that of the WT. On the contrary, *msh5* (1.45 ± 0.10, $P < 0.001$) and *fancm* (1.77 ± 0.02, $P < 0.001$) exhibited the opposite behavior, with a significantly lower fold change variation than the control. *zip4* (2.33 ± 0.26, $P = 0.741$) and *mus81* (1.89 ± 0.02, $P = 0.05$) were very similar to the WT and doubled their chiasma frequency after chromosome duplication.

© 2023 The Authors
New Phytologist © 2023 New Phytologist Foundation

14698137, 0, Downloaded from https://nph.onlinelibrary.wiley.com/doi/10.1111/nph.19366 by LEIBNIZ-INST. OF PLANT GENETICS AND CROP PLANT, Wiley Online Library on [23/11/2023]. See the Terms and Conditions (https://onlinelibrary.wiley.com/terms-and-conditions) on Wiley Online Library for rules of use; OA articles are governed by the applicable Creative Commons License

14698137, 0, Downloaded from https://nph.onlinelibrary.wiley.com/doi/10.1111/nph.19366 by LEIBNIZ-INST. OF PLANT GENETICS AND CROP PLANT, Wiley Online Library on [23/11/2023]. See the Terms and Conditions (https://onlinelibrary.wiley.com/terms-and-conditions) on Wiley Online Library for rules of use; OA articles are governed by the applicable Creative Commons License

Quantitative analysis of chromosomal configurations at metaphase I in tetraploid crossover-deficient mutants

We conducted FISH using rDNA probes on chromosomal spreads in metaphase I. The exhaustive cytological analysis of the morphology of the chromosomal configurations together with the position of the probe signals allowed us to infer the minimum number of chiasmata needed to produce the observed chromosomal associations (Sybenga, 1975; Santos *et al.*, 2003; Parra-Nunez *et al.*, 2020). In the diploids, we only observed bivalents and univalents in the genotypes studied (Figs S1, S2). By contrast, in the colchiploids, in addition to bivalents (II) and univalents (I), we observed trivalents (III) and quadrivalents (IV) (Figs 1, 2). In WT 4× cells, the chromosomes were predominantly associated as either II or IV. IV formation was more frequent than II formation and, very rarely, a group of four homologous chromosomes appeared as a III plus a I (16/186; 8.60%; Fig. 2c). This pattern of chromosomal configurations was also observed in the mutants with higher frequencies of chiasmata (*mus81* 4× and *fancm* 4×). The results from the ANOVA test ($F(2, 345) = 0.39$, $P = 0.680$) followed by Dunnett's *post hoc* test indicated that the II frequency per cell was not significantly different comparing either *mus81* 4× (2.46 ± 0.21, $P = 0.982$) or *fancm* 4× (2.22 ± 0.20, $P = 0.676$) with the WT (2.41 ± 0.15). However, significant differences were found in IV frequency ($F(2, 345) = 8.47$, $P < 0.001$). In this case, *mus81* 4× (3.62 ± 0.11, $P = 0.825$) showed no difference with the control (3.70 ± 0.08), but the frequency in *fancm* 4× (3.16 ± 0.12, $P < 0.001$) was significantly lower than that detected in the WT.

The III frequency in *fancm* 4× (0.63 ± 0.08) was higher than in the control (0.09 ± 0.02, $P < 0.001$), and the same was confirmed for I (1.02 ± 0.11 vs 0.11 ± 0.03, $P < 0.001$). In this mutant, we observed almost 50% of the cells with at least one III (46/96; 47.92%), and even > 10% with > 1 III (13/96; 13.54%). Cells with > 1 III were not detected in either the control or *mus81* 4×. *mus81* 4× showed no difference with the control in either I (0.29 ± 0.09, $P = 0.348$) or III (0.11 ± 0.04, $P > 0.999$). Therefore, *mus81* 4× did not differ from the control with respect to chromosomal configurations, while *fancm* 4× presented a decrease in the IV frequency due to the presence of more I and III.

In the other mutants analyzed, as expected due to their reduction in the chiasma frequency, we found significant differences with the WT in the frequency of III ($W(8.0, 190.3) = 15.75$, $P < 0.001$) and I ($W(8.0, 180.4) = 656$, $P < 0.001$; Fig. 2c). The mutants *asy1* 4× (0.54 ± 0.11, $P < 0.01$), *mer3* 4× (0.69 ± 0.13, $P < 0.001$), *hei10* 4× (0.56 ± 0.10, $P < 0.001$), and *mlh3* 4× (0.70 ± 0.10, $P < 0.001$) exhibited considerably higher frequencies than Col-0 4× (0.09 ± 0.02). However, *zip4* 4× (0.31 ± 0.11, $P = 0.334$) and *msh5* 4× (0.21 ± 0.04, $P = 0.064$) did not present an increase in III frequency, probably due to their very low chiasma frequencies. Accordingly, these mutants displayed the highest frequencies of I: *zip4* 4× (14.15 ± 0.56, $P < 0.001$) and *msh5* 4× (15.01 ± 0.26, $P < 0.001$). A significant increase in the I frequency with respect to the control was also observed in *asy1* 4× (10.63 ± 0.41, $P < 0.001$), *mer3* 4× (8.91 ± 0.61, $P < 0.001$), *hei10* 4× (9.53 ± 0.50, $P < 0.001$), and *mlh3* 4× (7.10 ± 0.36, $P < 0.001$).

The I frequency in *zmm* tetraploid mutants (*zip4* 4×, *msh5* 4×, *mer3* 4×, and *hei10* 4×) was also different from each other ($W(3.0, 79.66) = 51.10$, $P < 0.001$). We did not detect differences between *zip4* 4× and *msh5* 4× ($P = 0.669$), but these mutants showed more I than *hei10* 4×, and *mer3* 4× ($P < 0.001$ in all the cases). No differences were also detected between *hei10* 4× and *mer3* 4× ($P = 0.964$).

Analysis of class I crossovers in *fancm* 4× and Col-0 4×

As mentioned above, we detected a doubling of the number of chiasmata in the tetraploid control with respect to the diploid control, whereas the number of chiasmata did not double in *fancm* 4× with respect to *fancm* 2× (Fig. 2b). Immunolocalization of MLH1, a class I CO marker (Lhuissier *et al.*, 2007), was applied to determine the number of ZMM-dependent chiasmata in *fancm* 4× to get further insights into the behavior of this mutant after chromosome duplication. MLH1 foci at late pachynema were scored, using the transverse filament protein of the synaptonemal complex (ZYP1) as a cytological marker (Fig. 3). In *fancm* 2×, we did not find a significant variation with respect to the number of MLH1 foci in control cells (7.46 ± 0.38, $n = 24$ vs 8.33 ± 0.31, $n = 27$; $P = 0.390$; Fig. 3c), in agreement with previous studies (Crismani *et al.*, 2012; Knoll *et al.*, 2012). As in the diploid condition, no differences in the number of MLH1 foci were detected between *fancm* 4× and Col-0 4× ($P = 0.875$), since Col-0 4× displayed an average of 11.50 ± 0.76 ($n = 24$) and *fancm* 4× an average of 10.44 ± 0.66 ($n = 18$). Even though in the tetraploid mutants there was an increase in the number of MLH1 foci with respect to those observed in the diploid mutants (Col-0 2× vs Col-0 4×, $P < 0.01$; *fancm* 2× vs *fancm* 4×, $P < 0.01$), this increase was lower than that detected in chiasma frequency, not even reaching an increase of 50%. We further confirmed this result by performing a HEI10 immunolocalization. HEI10 is detected as large foci at sites of class I CO formation at late pachynema, colocalizing with MLH1 (Chelysheva *et al.*, 2012; Ziolkowski *et al.*, 2017; Morgan *et al.*, 2021). The results were very similar to those obtained for MLH1. An increase in HEI10 foci was detected in Col-0 4× (13.90 ± 0.65, $n = 21$) with respect to Col-0 2× (8.14 ± 0.21, $n = 77$; Welch's test, $t = 8.43$, $P < 0.001$), but the differences did not reach twofold (Fig. S4). This means that in the colchiploid class I COs did not increase in the same proportion as total COs did, suggesting changes in the ratio between both types of COs after chromosome duplication.

Expression analysis of meiotic genes in *hei10* 4×, *fancm* 4×, and Col-0 4×

To explore patterns of gene expression after chromosome duplication, we decided to assess transcription levels of some meiotic genes in *hei10* 4× (mutant that more than doubled the chiasma frequency after chromosome duplication), *fancm* 4× (mutant in which no doubling in chiasma frequency was reached after chromosome duplication), and the control (in which the chiasma

© 2023 The Authors
New Phytologist © 2023 New Phytologist Foundation

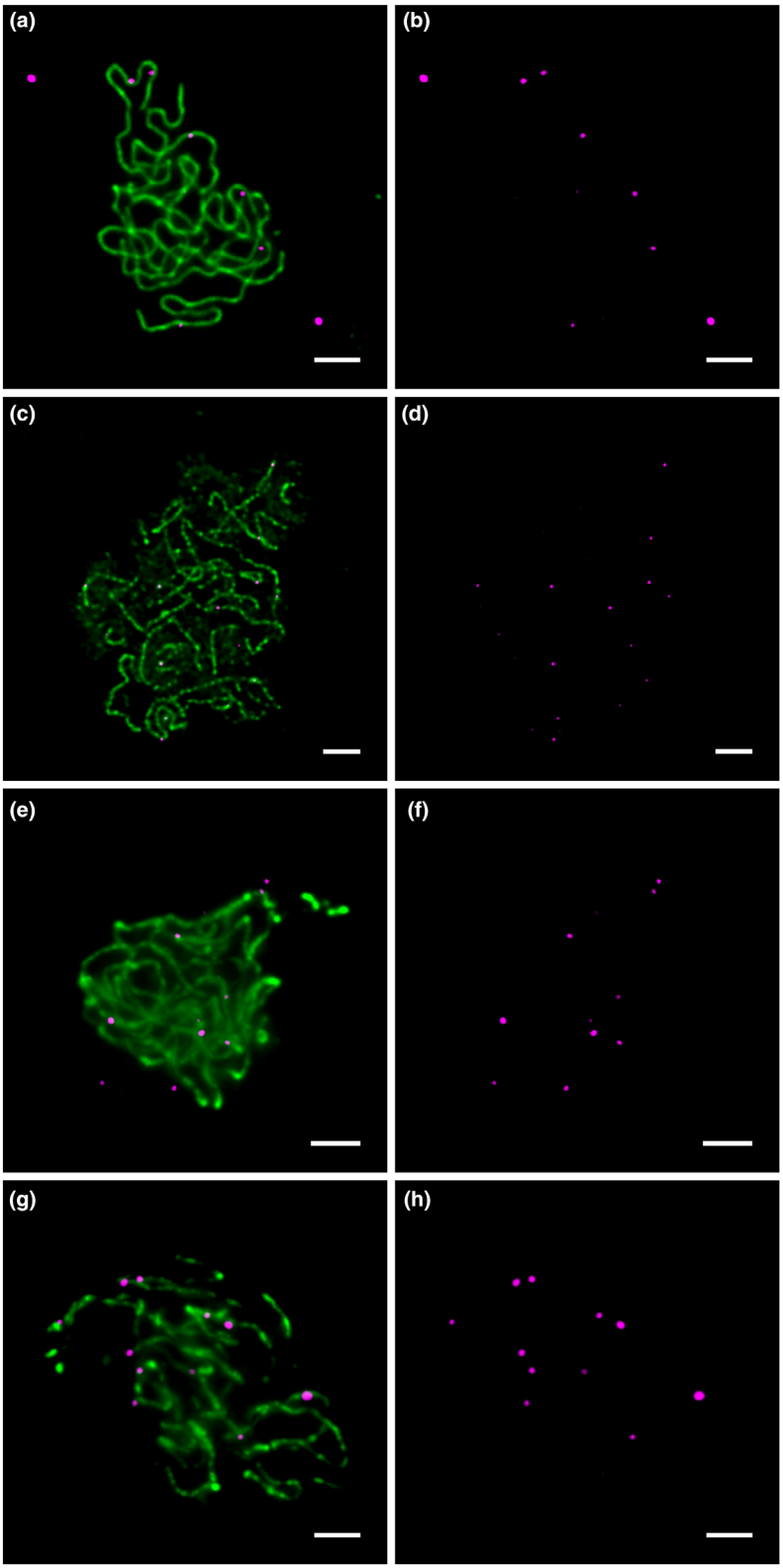

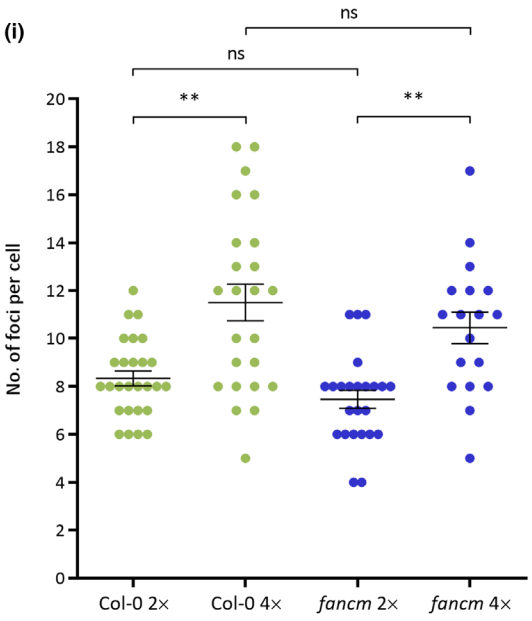

Fig. 3 Class I crossovers in *Arabidopsis thaliana* Columbia (Col-0) 4× and *fancm* 4× detected by MLH1. Double immunolocalization of ZYP1 (green) and MLH1 (magenta) on meiotic chromosome spreads. Representative examples of pachynemas from (a, b) Col-0 2×; (c, d) Col-0 4×; (e, f) *fancm* 2×; (g, h) *fancm* 4×. Bars, 5 μm. (i) Quantification of MLH1 foci in Col-0 2×, Col-0 4×, *fancm* 2×, and *fancm* 4×. Each dot represents an individual cell, bars indicate the mean, and error bars represent the SE of the mean. Welch's ANOVA showed statistical differences among the four lines ($W(3, 44.0) = 10.3$, $P < 0.001$). Dunnett's T3 *post hoc* test for pairwise comparisons showed statistical differences between Col-0 2× and Col-0 4×, and also between *fancm* 2× and *fancm* 4× (see the text for more details). However, the number of foci in *fancm* 2× is not significantly different from Col-0 2×. The same applies to *fancm* 4× and Col-0 4× (ns, nonsignificant; **, $P < 0.01$).

© 2023 The Authors
New Phytologist © 2023 New Phytologist Foundation

14698137, 0, Downloaded from https://nph.onlinelibrary.wiley.com/doi/10.1111/nph.19366 by LEIBNIZ-INST. OF PLANT GENETICS AND CROP PLANT, Wiley Online Library on [23/11/2023]. See the Terms and Conditions (https://onlinelibrary.wiley.com/terms-and-conditions) on Wiley Online Library for rules of use; OA articles are governed by the applicable Creative Commons License

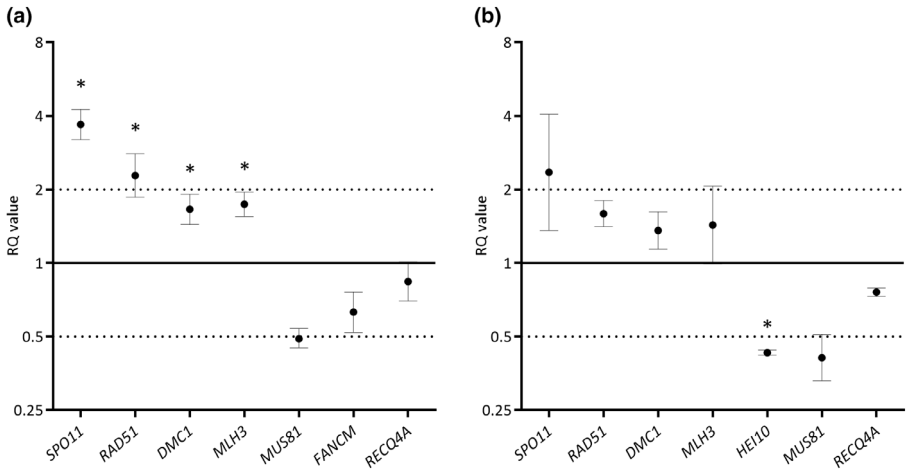

Fig. 4 RT-qPCR analyses for several meiotic genes involved in homologous recombination in *Arabidopsis thaliana hei10* 4× and *fancm* 4×. Relative transcription (RQ) levels of meiotic genes in samples from flower buds of (a) *fancm* 4× with respect to Columbia (Col-0) 4×, and (b) *hei10* 4× with respect to Col-0 4×. Error bars represent the SD of the RQ value. The solid lines indicate the RQ reference value (Col-0 4×). The dotted lines indicate the cut-offs corresponding to a fold change > 2-fold or < 0.5-fold (*Significant differences, 99% confidence interval).

frequency is doubled in the tetraploid). Several RT-qPCR analyses were conducted in flower bud samples from diploid and tetraploid individuals. Specifically, we evaluated mRNA levels of genes involved in the formation and processing of DSBs (*SPO11*, *RAD51*, and *DMC1*); class I CO formation (*MLH3* and *HEI10*); class II CO formation (*MUS81*); and CO/NCO regulation (*FANCM* and *RECQ4A*).

By comparing gene expression in diploids with that of their corresponding polyploids, we found hardly any variations in the genes selected in the study (Fig. S5). No changes were detected in the comparison between Col-0 2× and Col-0 4×. In the case of *hei10* 4×, only *SPO11* showed a very slight increase in expression in the tetraploid with respect to the diploid (RQ = 1.55). Regarding the comparison between *fancm* 2× and *fancm* 4×, we only detected a slight decrease in the *RECQ4A* transcription levels in *fancm* 4× (RQ = 0.81). The fold change was not > 2- or < 0.5-fold in any case.

However, we found more significant results in the comparison of *hei10* 4× with the tetraploid control. The expression of *SPO11* (RQ = 3.69), *RAD51* (RQ = 2.28), *DMC1* (RQ = 1.66), and *MLH3* (RQ = 1.74) presented a significant increase (Fig. 4). These changes in gene expression do not seem to be due to the genetic background itself, since in the comparison of *hei10* 2× with Col-0 2× we did not find changes in mRNA levels for these genes (Fig. S5). On the contrary, the > 2-fold increase in expression of *SPO11* and *RAD51* in *hei10* 4× appears to be meiosis-specific, as neither of these genes showed changes in mRNA levels in the seedling samples (*SPO11*: RQ = 1.11; *RAD51*: RQ = 1.17).

Finally, *fancm* 4× exhibited significantly reduced mRNA levels for *HEI10* (RQ = 0.43) with respect to Col-0 4× (Fig. 4), but this reduction was also detected in seedling samples (RQ = 0.17). *HEI10* also showed a reduction in expression in the diploid mutant *fancm* 2× with respect to the control (RQ = 0.31; Fig. S5). Therefore, this variation in *HEI10* mRNA levels would not be specific to chromosome duplication and would be an alteration associated with the *fancm* mutation.

Discussion

Polyploidy affects chromosomal behavior during meiosis. It has fundamental consequences on this cell division since, due to the presence of four homologous chromosomes, multivalents can be formed in addition to the bivalents observed in a diploid genetic background. This situation is even more favored in autopolyploids than in allopolyploids since there are no differentiated subgenomes. Indeed, these two types of polyploids use different strategies during the meiotic stabilization process (Bomblies, 2023). Polyploidy may be useful in the study of mutants whose frequency of CO formation is altered. The presence of more than two homologous chromosomes that can pair, synapse, and recombine with each other, together with the fact that the gene dose is increased, and the expression of some genes altered, may contribute to a better understanding of the potential effects of meiotic mutations. The meiotic mutants can exhibit new phenotypes in addition to their behavior in diploid condition. For example, Arabidopsis autotetraploid mutants for NSE2 and NSE4A (subunits of the STRUCTURAL MAINTENANCE OF CHROMOSOMES 5/6, SMC5/6) had more severe meiotic defects and generate aneuploid offspring (Yang *et al.*, 2021). Recently, Desjardins *et al.* (2022) have demonstrated that in wheat, an allopolyploid, FANCM not only suppresses class II COs, but also promotes class I COs. In the current work, we have analyzed autopolyploids and found that there are Arabidopsis mutants in which chromosome doubling is accompanied by a chiasma frequency duplication (*zip4*, *mus81*), as in the control. In other CO-deficient mutants, the presence of additional homologous chromosomes leads to a higher-than-expected increase in chiasma frequency (*asy1*, *mer3*, *hei10*, and *mlh3*). Finally, there are other mutants in which the rise in chiasma frequency produced by the presence of extrachromosomal sets is less than doubled (*msh5* and *fancm*; Fig. 2).

Polyploidy reveals differences in chiasma frequencies among *zmm* mutants

The ZMM epistatic group defined by Börner *et al.* (2004) is composed in Arabidopsis by *ZIP4*, *MSH4/5*, *MER3*, and *HEI10*, among others. The corresponding mutants suppress *c.* 85% of the COs (Higgins *et al.*, 2004, 2008b; Chen *et al.*, 2005; Chelysheva *et al.*, 2007, 2012), except *mer3* which suppresses *c.* 75% (Mercier *et al.*, 2005). In our analyses, we have confirmed this

© 2023 The Authors
New Phytologist © 2023 New Phytologist Foundation

14698137, 0, Downloaded from https://nph.onlinelibrary.wiley.com/doi/10.1111/nph.19366 by LEIBNIZ-INST. OF PLANT GENETICS AND CROP PLANT, Wiley Online Library on [23/11/2023]. See the Terms and Conditions (https://onlinelibrary.wiley.com/terms-and-conditions) on Wiley Online Library for rules of use; OA articles are governed by the applicable Creative Commons License

result, since *mer3* 2× presented a significantly higher chiasma frequency than that of the other three *zmm* mutants analyzed (Fig. S2). Chen *et al.* (2005) suggested that other genes may have functions overlapping with those of *MER3*. This difference in chiasma frequency persisted in colchiploids, although in this case, *hei10* 4× did not differ in the number of chiasmata from *mer3* 4×. *zip4* 4× and *msh5* 4× showed the lowest chiasma frequencies and the highest frequencies of univalents (Fig. 2). In addition, in the current study, only *mer3* and *hei10* mutants increase their chiasma frequency > 2-fold after chromosome duplication (Fig. 2). It is therefore possible that *ZMM* genes are not equivalent in the interference-sensitive CO pathway, and MER3 and HEI10 may act downstream of the other ZMM proteins. In this context, Shen *et al.* (2012) reported that ZIP4 and MER3 work cooperatively in rice meiosis, but their specific contribution to CO formation is not identical. ZIP4 could be playing an earlier function, contributing to a proper environment to recruit other proteins required to mature recombination intermediates. Furthermore, Luo *et al.* (2013) found that MSH5 is needed for the correct localization of ZIP4 and MER3 during rice prophase I. Further investigations using double mutants are required to clarify the implication of these proteins in the main CO pathway in Arabidopsis.

The peculiar behavior of *hei10* after chromosome duplication could be related to the coarsening dynamics of the protein and its function in CO positioning and interference (Morgan *et al.*, 2021; Durand *et al.*, 2022). In this mutant, when there is more than one homologous chromosome, despite the absence of HEI10, more chiasma formation may occur than when other ZMM are absent. Most likely, these additional chiasmata in *hei10* 4× belong to class II, as revealed by chiasma distribution analyses (Fig. S3). Interestingly, the proportion of class I and class II COs varies after chromosome duplication, as shown by the results obtained for Col-0 4× (Figs 3, S4). At the diploid level, class I COs would represent *c.* 85% of the total amount of chiasmata, whereas in the tetraploid this percentage drops to 60% (12 MLH1 foci and 20 chiasmata). In *zmm* mutants, the formation of class I COs is compromised, but the number of class II COs in *hei10* is greater than that in *zip4* or *msh5* (only in tetraploids).

Another factor to consider is the possible variation in gene expression because of chromosome duplication. For example, in autotetraploid *Brassica rapa* 6.3% of the genes differentially expressed with respect to the diploid in immature buds have a meiotic function (Braynen *et al.*, 2017). *SPO11* and genes involved in DSB formation displayed a similar expression level in both autotetraploid and diploid *B. rapa*, whereas the recombinase *DMC1* is significantly downregulated in the autotetraploid. On the contrary, the genes *ZYP1* (transverse filaments of the synaptonemal complex) and *SYN1* (meiosis-specific cohesion) are upregulated in autotetraploid *Arabidopsis arenosa* and *B. rapa* (Yant *et al.*, 2013; Braynen *et al.*, 2017). For the genes analyzed in this study, we have found that there are no variations in expression levels after polyploidy in the WT (Fig. S5). However, in *hei10* 4× we detected a meiosis-specific enhanced expression of *SPO11* and *RAD51* (and of *DMC1* and *MLH3*, although < 2-fold in this case). Although this variation does not explain the cytogenetic behavior of the mutant after chromosome duplication, it reveals that gene expression regulation in *hei10* after chromosome doubling is different from that of the control. It is possible that in this mutant, problems in CO formation lead to a more prolonged formation of DSBs over time, as occurs in yeast (Thacker *et al.*, 2014). Perhaps this would increase the number of class II COs above what is possible in other *ZMM* mutants. Further experiments would be needed to confirm this.

mlh3 4× and *mus81* 4× mutants behave similarly to *mer3* 4× and Col-0 4×, respectively

Chromosomal analysis of *mlh3* 4× revealed that this mutant is very similar to *mer3* 4×. In diploid condition, the mean number of chiasmata of *mlh3* 2× is similar to that of *mer3* 2× (Chen *et al.*, 2005; Mercier *et al.*, 2005; Jackson *et al.*, 2006). The colchiploids of these mutants were also very similar with respect to the mean chiasma frequency, the fold change between the corresponding tetraploid and diploid chiasma frequencies, and the chromosome configurations observed at metaphase I (Fig. 2). In *mlh3* 4×, as well as in *mer3* 4×, after chromosome duplication the number of chiasmata increased > 2-fold. As in the case of *mer3* 4×, this may be due to the different proportion of class I/class II COs in tetraploids (Fig. 3).

On the contrary, *mus81* 2× and *mus81* 4× presented similar chiasma frequencies compared with their respective controls (Figs 2, S2). Besides, *mus81* 4× and Col-0 4× displayed similar numbers for the different chromosome configurations observed at metaphase I (Fig. 2). These results and the increase in the proportion of class II COs in Col-0 4× (Fig. 3) seem to indicate that there are alternative pathways, MUS81-independent, involved in the formation of class II COs. Kurzbauer *et al.* (2018) proposed that some of the recombination intermediates that are processed by MUS81 could be processed by FANCD2 in *mus81*. Interestingly, this protein, FANCD2, is also involved in regulating the distribution of class I COs among chromosomes (Li *et al.*, 2021).

Chiasma frequency and chromosomal configurations are altered in *fancm* 4× with respect to Col-0 4×

The FANCM helicase limits class II COs in plants by unwinding recombination intermediates. In Arabidopsis, the mutation *fancm* hardly affects bivalent formation (Crismani *et al.*, 2012; Knoll *et al.*, 2012). However, in allopolyploid wheat, FANCM is required for CO assurance, since 64% of metaphase I cells in the tetraploid and 37% in the hexaploid show univalents (Desjardins *et al.*, 2022). We have also observed differences in the chromosomal configurations of *fancm* 4× with respect to those observed in Col-0 4× (Fig. 2). We have detected a significant increase in univalents and trivalents at the expense of a decrease in quadrivalents. It would be interesting to analyze whether the increase in the frequency of univalents and trivalents also occurs in tetraploid mutants defective in anti-CO proteins involved in different pathways to FANCM, such as *recq4a recq4b* or *fidgl1* (Girard *et al.*, 2015; Séguéla-Arnaud *et al.*, 2015). In addition, *fancm* 4× displayed a significant decrease in chiasma numbers with respect

© 2023 The Authors
New Phytologist © 2023 New Phytologist Foundation

14698137, 0, Downloaded from https://nph.onlinelibrary.wiley.com/doi/10.1111/nph.19366 by LEIBNIZ-INST. OF PLANT GENETICS AND CROP PLANT, Wiley Online Library on [23/11/2023]. See the Terms and Conditions (https://onlinelibrary.wiley.com/terms-and-conditions) on Wiley Online Library for rules of use; OA articles are governed by the applicable Creative Commons License

to the tetraploid WT (Fig. 2). Immunolocalization results show that the number of MLH1 foci, that is class I CO, in *fancm* does not change with respect to the control (neither in diploid nor in tetraploid condition), suggesting that the chiasma reduction in *fancm* 4× is probably due to a loss of class II COs (Fig. 3). On the contrary, the modification in the type of chromosomal configurations could also point to the distribution pattern of class I COs being altered in *fancm* 4×, as suggested for *fancm* 2× (Li *et al.*, 2021). This function of FANCM could be related to the reduction in *HEI10* expression detected in RT-qPCR analyses. This reduction was present in both *fancm* 2× and *fancm* 4× (Figs 4, S5).

The increase in chiasma frequency is higher-than-expected in *asy1* 4×

In *asy1*, chiasma frequency is more than doubled after chromosome duplication, in contrast to the control (2.87 vs 1.96, Fig. 2). Tian *et al.* (2011) reported an increase in the fertility levels of *asy1* 4× compared with its diploid counterpart. These results might indicate an advantage in *asy* 4× over *asy* 2×. Indeed, *ASY1* has been identified as a candidate gene for meiotic stabilization in *A. arenosa* tetraploids (Morgan *et al.*, 2020). In addition, ASY1 is involved in promoting spaced CO formation along the chromosomes and functions as a gene dosage-dependent antagonist of telomere-led recombination (Lambing *et al.*, 2020; Pochon *et al.*, 2022). The increased proportion of class II COs in tetraploids and the altered distribution of class I COs due to the absence of ASY1 could explain the cytological behavior of *asy1* 4× (Fig. 2). Despite pairing and synapsis are severely compromised in *asy1*, telomere clustering is not affected, and recombination becomes largely restricted to telomeric and subtelomeric regions (Sanchez-Moran *et al.*, 2007; Lambing *et al.*, 2020; Pochon *et al.*, 2022). In this landscape, an increased chance of recombination with a homologous chromosome (in *asy1* 4× each chromosome has three potential partners to recombine with) could explain the increased chiasma frequency observed in *asy1* 4× (Fig. 2).

Concluding remarks

Cytogenetic studies in *A. thaliana* meiotic mutants have significantly contributed to providing essential knowledge on the functionality of key meiotic proteins (Gutiérrez Pinzón *et al.*, 2021). *Arabidopsis thaliana* is a powerful model, but it should be considered that it is a diploid species and that most crops are polyploid species. Owing to the presence of more than two homologous chromosomes, polyploid meiosis faces a great variety of challenges, and in this context, mutations in meiotic genes may have a different effect than in a situation where each chromosome has only one partner to recombine with, as evidenced by the results obtained. This work provides an opportunity to test whether particular mutants may enable the formation of stable polyploids. This can lay the groundwork for future studies about the effects of such mutations in autopolyploid crops, which offer more complexities for cytogenetic analyses.

Acknowledgements

We thank Bianca Martín, M. Carmen Moreno, and José Barrios for their technical assistance. Primary antibodies were kindly provided by Chris Franklin (University of Birmingham, UK). This research was supported by the European Union (Marie Curie ITN, COMREC 606956) to MP and the Ministry of Economy and Competitiveness of Spain (AGL2015-67349-P) to JLS. MP acknowledges the current support of the Ministry of Science and Innovation (PID2020-118038GB-I00) and European Union (TED2021-131852B-I00/AEI/10.13039/501100011033/Unión Europea NextGeneration EU/PRTR).

Competing interests

None declared.

Author contributions

MP and JLS designed the research project. PP-N acquired, analyzed, and interpreted the data for the work. NF-J and MP-P contributed to the collection of the results and preparation of figures. PP-N and MP wrote the manuscript. JLS and ES-M revised the content of the manuscript critically. All authors read and approved the final manuscript. MP and JLS contributed equally to this work.

ORCID

Nadia Fernández-Jiménez https://orcid.org/0000-0002-4196-0134
Miguel Pachon-Penalba https://orcid.org/0000-0002-1499-0880
Pablo Parra-Nunez https://orcid.org/0000-0003-3060-6452
Mónica Pradillo https://orcid.org/0000-0001-6625-6015
Eugenio Sanchez-Moran https://orcid.org/0000-0002-7417-0024
Juan Luis Santos https://orcid.org/0000-0003-4475-9628

Data availability

The data that support the findings of this study are available in the Supplementary Information. Raw data can be obtained from the data repository 'Docta Complutense': https://hdl.handle.net/20.500.14352/88106.

References

Armstrong SJ, Caryl AP, Jones GH, Franklin FC. 2002. Asy1, a protein required for meiotic chromosome synapsis, localizes to axis-associated chromatin in *Arabidopsis* and *Brassica*. *Journal of Cell Science* **115**: 3645–3655.

Armstrong SJ, Sanchez-Moran E, Franklin FC. 2009. Cytological analysis of *Arabidopsis thaliana* meiotic chromosomes. *Methods in Molecular Biology* **558**: 131–145.

Baker SM, Plug AW, Prolla TA, Bronner CE, Harris AC, Yao X, Christie DM, Monell C, Arnheim N, Bradley A *et al.* 1996. Involvement of mouse Mlh1 in DNA mismatch repair and meiotic crossing over. *Nature Genetics* **13**: 336–342.

© 2023 The Authors
New Phytologist © 2023 New Phytologist Foundation

14698137, 0, Downloaded from https://nph.onlinelibrary.wiley.com/doi/10.1111/nph.19366 by LEIBNIZ-INST. OF PLANT GENETICS AND CROP PLANT, Wiley Online Library on [23/11/2023]. See the Terms and Conditions (https://onlinelibrary.wiley.com/terms-and-conditions) on Wiley Online Library for rules of use; OA articles are governed by the applicable Creative Commons License

Berchowitz LE, Francis KE, Bey AL, Copenhaver GP. 2007. The role of AtMUS81 in interference-insensitive crossovers in *A. thaliana*. *PLoS Genetics* **3**: e132.

Bomblies K. 2023. Learning to tango with four (or more): the molecular basis of adaptation to polyploid meiosis. *Plant Reproduction* **36**: 107–124.

Bomblies K, Jones G, Franklin C, Zickler D, Kleckner N. 2016. The challenge of evolving stable polyploidy: could an increase in "crossover interference distance" play a central role? *Chromosoma* **125**: 287–300.

Börner GV, Kleckner N, Hunter N. 2004. Crossover/noncrossover differentiation, synaptonemal complex formation, and regulatory surveillance at the leptotene/zygotene transition of meiosis. *Cell* **117**: 29–45.

Braynen J, Yang Y, Wei F, Cao G, Shi G, Tian B, Zhang X, Jia H, Wei X, Wei Z. 2017. Transcriptome analysis of floral buds deciphered an irregular course of meiosis in polyploid *Brassica rapa*. *Frontiers in Plant Science* **8**: 768.

Campell BR, Song Y, Posch TE, Cullis CA, Town CD. 1992. Sequence and organization of 5S ribosomal RNA-encoding genes of *Arabidopsis thaliana*. *Gene* **112**: 225–228.

Chambon A, West A, Vezon D, Horlow C, De Muyt A, Chelysheva L, Ronceret A, Darbyshire A, Osman K, Heckmann S *et al.* 2018. Identification of ASYNAPTIC4, a component of the meiotic chromosome axis. *Plant Physiology* **178**: 233–246.

Chelysheva L, Gendrot G, Vezon D, Doutriaux MP, Mercier R, Grelon M. 2007. Zip4/Spo22 is required for class I CO formation but not for synapsis completion in *Arabidopsis thaliana*. *PLoS Genetics* **3**: e83.

Chelysheva L, Vezon D, Chambon A, Gendrot G, Pereira L, Lemhemdi A, Vrielynck N, Le Guin S, Novatchkova M, Grelon M. 2012. The *Arabidopsis* HEI10 is a new ZMM protein related to Zip3. *PLoS Genetics* **8**: e1002799.

Chen C, Zhang W, Timofejeva L, Gerardin Y, Ma H. 2005. The Arabidopsis *ROCK-N-ROLLERS* gene encodes a homolog of the yeast ATP-dependent DNA helicase MER3 and is required for normal meiotic crossover formation. *The Plant Journal* **43**: 321–334.

Copenhaver GP, Housworth EA, Stahl FW. 2002. Crossover interference in Arabidopsis. *Genetics* **160**: 1631–1639.

Crismani W, Girard C, Froger N, Pradillo M, Santos JL, Chelysheva L, Copenhaver GP, Horlow C, Mercier R. 2012. FANCM limits meiotic crossovers. *Science* **336**: 1588–1590.

Desjardins SD, Simmonds J, Guterman I, Kanyuka K, Burridge AJ, Tock AJ, Sanchez-Moran E, Franklin FCH, Henderson IR, Edwards KJ *et al.* 2022. FANCM promotes class I interfering crossovers and suppresses class II non-interfering crossovers in wheat meiosis. *Nature Communications* **13**: 3644.

Durand S, Lian Q, Jing J, Ernst M, Grelon M, Zwicker D, Mercier R. 2022. Joint control of meiotic crossover patterning by the synaptonemal complex and HEI10 dosage. *Nature Communications* **13**: 5999.

Ferdous M, Higgins JD, Osman K, Lambing C, Roitinger E, Mechtler K, Armstrong SJ, Perry R, Pradillo M, Cuñado N *et al.* 2012. Inter-homolog crossing-over and synapsis in *Arabidopsis* meiosis are dependent on the chromosome axis protein AtASY3. *PLoS Genetics* **8**: e1002507.

Fernandes JB, Duhamel M, Seguéla-Arnaud M, Froger N, Girard C, Choinard S, Solier V, De Winne N, De Jaeger G, Gevaert K *et al.* 2018. FIGL1 and its novel partner FLIP form a conserved complex that regulates homologous recombination. *PLoS Genetics* **14**: e1007317.

Franklin FC, Higgins JD, Sanchez-Moran E, Armstrong SJ, Osman KE, Jackson N, Jones GH. 2006. Control of meiotic recombination in *Arabidopsis*: role of the *MutL* and *MutS* homologues. *Biochemical Society Transactions* **34**: 542–544.

Fransz P, Armstrong S, Alonso-Blanco C, Fischer TC, Torres-Ruiz RA, Jones G. 1998. Cytogenetics for the model system *Arabidopsis thaliana*. *The Plant Journal* **13**: 867–876.

Gerlach WL, Bedbrook JR. 1979. Cloning and characterization of ribosomal RNA genes from wheat and barley. *Nucleic Acids Research* **7**: 1869–1885.

Girard C, Chelysheva L, Choinard S, Froger N, Macaisne N, Lemhemdi A, Mazel J, Crismani W, Mercier R. 2015. AAA-ATPase FIDGETIN-LIKE 1 and helicase FANCM antagonize meiotic crossovers by distinct mechanisms. *PLoS Genetics* **11**: e1005369.

Girard C, Crismani W, Froger N, Mazel J, Lemhemdi A, Horlow C, Mercier R. 2014. FANCM-associated proteins MHF1 and MHF2, but not the other Fanconi anemia factors, limit meiotic crossovers. *Nucleic Acids Research* **42**: 9087–9095.

Gutiérrez Pinzón Y, González Kise JK, Rueda P, Ronceret A. 2021. The formation of bivalents and the control of plant meiotic recombination. *Frontiers in Plant Science* **12**: 717423.

Higgins JD, Armstrong SJ, Franklin FC, Jones GH. 2004. The *Arabidopsis MutS* homolog *AtMSH4* functions at an early step in recombination: evidence for two classes of recombination in *Arabidopsis*. *Genes & Development* **18**: 2557–2570.

Higgins JD, Buckling EF, Franklin FC, Jones GH. 2008a. Expression and functional analysis of *AtMUS81* in Arabidopsis meiosis reveals a role in the second pathway of crossing-over. *The Plant Journal* **54**: 152–162.

Higgins JD, Sanchez-Moran E, Armstrong SJ, Jones GH, Franklin FC. 2005. The *Arabidopsis* synaptonemal complex protein ZYP1 is required for chromosome synapsis and normal fidelity of crossing over. *Genes & Development* **19**: 2488–2500.

Higgins JD, Vignard J, Mercier R, Pugh AG, Franklin FC, Jones GH. 2008b. AtMSH5 partners AtMSH4 in the class I meiotic crossover pathway in *Arabidopsis thaliana*, but is not required for synapsis. *The Plant Journal* **55**: 28–39.

Higgins JD, Wright KM, Bomblies K, Franklin FCH. 2014. Cytological techniques to analyze meiosis in *Arabidopsis arenosa* for investigating adaptation to polyploidy. *Frontiers in Plant Science* **4**: 546.

Hsieh AYY, Saberi S, Ajaykumar A, Hukezalie K, Gadawski I, Sattha B, Côté HCF. 2016. Optimization of a relative telomere length assay by monochromatic multiplex real-time quantitative PCR on the LightCycler 480: sources of variability and quality control considerations. *Journal of Molecular Diagnostics* **18**: 425–437.

Jackson N, Sanchez-Moran E, Buckling E, Armstrong SJ, Jones GH, Franklin FC. 2006. Reduced meiotic crossovers and delayed prophase I progression in AtMLH3-deficient Arabidopsis. *EMBO Journal* **25**: 1315–1323.

Knoll A, Higgins JD, Seeliger K, Reha SJ, Dangel NJ, Bauknecht M, Schröpfer S, Franklin FC, Puchta H. 2012. The Fanconi anemia ortholog FANCM ensures ordered homologous recombination in both somatic and meiotic cells in *Arabidopsis*. *Plant Cell* **24**: 1448–1464.

Kurzbauer MT, Pradillo M, Kerzendorfer C, Sims J, Ladurner R, Oliver C, Janisiw MP, Mosiolek M, Schweizer D, Copenhaver GP *et al.* 2018. *Arabidopsis thaliana* FANCD2 promotes meiotic crossover formation. *Plant Cell* **30**: 415–428.

Lambing C, Kuo PC, Tock AJ, Topp SD, Henderson IR. 2020. ASY1 acts as a dosage-dependent antagonist of telomere-led recombination and mediates crossover interference in *Arabidopsis*. *Proceedings of the National Academy of Sciences, USA* **117**: 13647–13658.

Lambing C, Osman K, Nuntasoontorn K, West A, Higgins JD, Copenhaver GP, Yang J, Armstrong SJ, Mechtler K, Roitinger E *et al.* 2015. Arabidopsis PCH2 mediates meiotic chromosome remodeling and maturation of crossovers. *PLoS Genetics* **11**: e1005372.

Lhuissier FGP, Offenberg HH, Wittich PE, Vischer NOE, Heyting C. 2007. The mismatch repair protein MLH1 marks a subset of strongly interfering crossovers in tomato. *Plant Cell* **19**: 862–876.

Li X, Zhang J, Huang J, Xu J, Chen Z, Copenhaver GP, Wang Y. 2021. Regulation of interference-sensitive crossover distribution ensures crossover assurance in *Arabidopsis*. *Proceedings of the National Academy of Sciences, USA* **118**: e2107543118.

Livak KJ, Schmittgen TD. 2001. Analysis of relative gene expression data using real-time quantitative PCR and the $2^{-\Delta\Delta Ct}$ method. *Methods* **25**: 402–408.

Luo Q, Tang D, Wang M, Luo W, Zhang L, Qin B, Shen Y, Wang K, Li Y, Cheng Z. 2013. The role of OsMSH5 in crossover formation during rice meiosis. *Molecular Plant* **6**: 729–742.

Mercier R, Jolivet S, Vezon D, Huppe E, Chelysheva L, Giovanni M, Nogué F, Doutriaux MP, Horlow C, Grelon M *et al.* 2005. Two meiotic crossover classes cohabit in *Arabidopsis*: one is dependent on *MER3*, whereas the other one is not. *Current Biology* **15**: 692–701.

Mercier R, Mézard C, Jenczewski E, Macaisne N, Grelon M. 2015. The molecular biology of meiosis in plants. *Annual Review of Plant Biology* **66**: 297–327.

Morgan C, Fozard JA, Hartley M, Henderson IR, Bomblies K, Howard M. 2021. Diffusion-mediated HEI10 coarsening can explain meiotic crossover positioning in *Arabidopsis*. *Nature Communications* **12**: 4674.

Morgan C, Zhang H, Henry CE, Franklin FCH, Bomblies K. 2020. Derived alleles of two axis proteins affect meiotic traits in autotetraploid *Arabidopsis*

© 2023 The Authors
New Phytologist © 2023 New Phytologist Foundation

14698137, 0, Downloaded from https://nph.onlinelibrary.wiley.com/doi/10.1111/nph.19366 by LEIBNIZ-INST. OF PLANT GENETICS AND CROP PLANT, Wiley Online Library on [23/11/2023]. See the Terms and Conditions (https://onlinelibrary.wiley.com/terms-and-conditions) on Wiley Online Library for rules of use; OA articles are governed by the applicable Creative Commons License

arenosa. *Proceedings of the National Academy of Sciences of the USA* **117**: 8980–8988.

Osman K, Higgins JD, Sanchez-Moran E, Armstrong SJ, Franklin FC. 2011. Pathways to meiotic recombination in *Arabidopsis thaliana*. *New Phytologist* **190**: 523–544.

Parra-Nunez P, Pradillo M, Santos JL. 2019. Competition for chiasma formation between identical and homologous (but not identical) chromosomes in synthetic autotetraploids of *Arabidopsis thaliana*. *Frontiers in Plant Science* **9**: 1924.

Parra-Nunez P, Pradillo M, Santos JL. 2020. How to perform an accurate analysis of metaphase I chromosome configurations in autopolyploids of *Arabidopsis thaliana*. *Methods in Molecular Biology* **2061**: 25–36.

Pecinka A, Fang W, Rehmsmeier M, Levy AA, Mittelsten SO. 2011. Polyploidization increases meiotic recombination frequency in Arabidopsis. *BMC Biology* **9**: 24.

Pochon G, Henry IM, Yang C, Lory N, Fernández-Jiménez N, Böwer F, Hu B, Carstens L, Tsai HT, Pradillo M *et al.* 2022. The Arabidopsis Hop1 homolog ASY1 mediates cross-over assurance and interference. *Proceedings of the National Academy of Sciences, Nexus* **2**: pgac302.

Riedel G, Rüdrich U, Fekete-Drimusz N, Manns MP, Vondran FWR, Bock M. 2014. An extended ΔC_t-method facilitating normalisation with multiple reference genes suited for quantitative RT-PCR analyses of human hepatocyte-like cells. *PLoS ONE* **9**: e93031.

Roelens B, Schvarzstein M, Villeneuve AM. 2015. Manipulation of karyotype in *Caenorhabditis elegans* reveals multiple inputs driving pairwise chromosome synapsis during meiosis. *Genetics* **201**: 1363–1379.

Ross KJ, Fransz P, Armstrong SJ, Vizir I, Mulligan B, Franklin FC, Jones GH. 1997. Cytological characterization of four meiotic mutants of *Arabidopsis* isolated from T-DNA-transformed lines. *Chromosome Research* **5**: 551–559.

Sanchez-Moran E, Armstrong SJ, Santos JL, Franklin FC, Jones GH. 2001. Chiasma formation in *Arabidopsis thaliana* accession Wassileskija and in two meiotic mutants. *Chromosome Research* **9**: 121–128.

Sanchez-Moran E, Santos JL, Jones GH, Franklin FC. 2007. ASY1 mediates AtDMC1-dependent interhomolog recombination during meiosis in *Arabidopsis*. *Genes & Development* **21**: 2220–2233.

de los Santos T, Hunter N, Lee C, Larkin B, Loidl J, Hollingsworth NM. 2003. The *Mus81*/*Mms4* endonuclease acts independently of double-Holliday junction resolution to promote a distinct subset of crossovers during meiosis in budding yeast. *Genetics* **164**: 81–94.

Santos JL, Alfaro D, Sanchez-Moran E, Armstrong SJ, Franklin FC, Jones GH. 2003. Partial diploidization of meiosis in autotetraploid *Arabidopsis thaliana*. *Genetics* **165**: 1533–1540.

Séguéla-Arnaud M, Choinard S, Larchevêque C, Girard C, Froger N, Crismani W, Mercier R. 2017. RMI1 and TOP3α limit meiotic CO formation through their C-terminal domains. *Nucleic Acids Research* **45**: 1860–1871.

Séguéla-Arnaud M, Crismani W, Larchevêque C, Mazel J, Froger N, Choinard S, Lemhemdi A, Macaisne N, Van Leene J, Gevaert K *et al.* 2015. Multiple mechanisms limit meiotic crossovers: TOP3α and two BLM homologs antagonize crossovers in parallel to FANCM. *Proceedings of the National Academy of Sciences, USA* **112**: 4713–4718.

Shen Y, Tang D, Wang K, Wang M, Huang J, Luo W, Luo Q, Hong L, Li M, Cheng Z. 2012. ZIP4 in homologous chromosome synapsis and crossover formation in rice meiosis. *Journal of Cell Science* **125**: 2581–2591.

Sybenga J. 1975. *Meiotic configurations*. Berlin, Germany: Springer.

Thacker D, Mohibullah N, Zhu X, Keeney S. 2014. Homologue engagement controls meiotic DNA break number and distribution. *Nature* **510**: 241–246.

Tian B, Yan B, Gao JY, Si YH, Zang X. 2011. Dissecting 2 meiotic mutations (*dmc1* and *asy1*) in artificial autopolyploid *Arabidopsis thaliana*. *Cytologia* **76**: 411–423.

Wang H, Wang J, Jiang J, Chen S, Guan Z, Liao Y, Chen F. 2014. Reference genes for normalizing transcription in diploid and tetraploid Arabidopsis. *Scientific Reports* **4**: 6781.

Wang Y, Copenhaver GP. 2018. Meiotic recombination: mixing it up in plants. *Annual Review of Plant Biology* **69**: 577–609.

Yang F, Fernández Jiménez N, Majka J, Pradillo M, Pecinka A. 2021. Structural maintenance of chromosomes 5/6 complex is necessary for tetraploid genome stability in *Arabidopsis thaliana*. *Frontiers in Plant Science* **12**: 748252.

Yant L, Hollister JD, Wright KM, Arnold BJ, Higgins JD, Franklin FCH, Bomblies K. 2013. Meiotic adaptation to genome duplication in *Arabidopsis arenosa*. *Current Biology* **23**: 2151–2156.

Yu Z, Haage K, Streit VE, Gierl A, Torres Ruiz RA. 2009. A large number of tetraploid *Arabidopsis thaliana* lines, generated by a rapid strategy, reveal high stability of neo-tetraploids during consecutive generations. *Theoretical and Applied Genetics* **118**: 1107–1119.

Ziolkowski PA, Underwood CJ, Lambing C, Martinez-Garcia M, Lawrence EJ, Ziolkowska L, Griffin C, Choi K, Franklin FC, Martienssen RA *et al.* 2017. Natural variation and dosage of the HEI10 meiotic E3 ligase control *Arabidopsis* crossover recombination. *Genes & Development* **31**: 306–317.

Supporting Information

Additional Supporting Information may be found online in the Supporting Information section at the end of the article.

Fig. S1 Cytological analysis of *Arabidopsis thaliana* male meiocytes at metaphase I in mutants with altered crossover frequency.

Fig. S2 Mean cell chiasma frequencies and chromosomal configurations at metaphase I in *Arabidopsis thaliana* mutants with altered crossover frequency.

Fig. S3 Observed and Poisson-predicted distributions of chiasma frequency per cell in *Arabidopsis thaliana hei10* 2× and *hei10* 4× and their corresponding controls.

Fig. S4 Class I crossovers in *Arabidopsis thaliana* Col-0 4× detected by HEI10.

Fig. S5 RT-qPCR analyses for several meiotic genes involved in homologous recombination in *Arabidopsis thaliana hei10* 2×, *hei10* 4×, *fancm* 2×, and *fancm* 4×.

Table S1 PCR primers used for genotyping.

Table S2 Genes analyzed by RT-qPCR, UPL probes, and primers.

Table S3 Comparison of the mean cell chiasma frequency among the different *Arabidopsis thaliana zmm* mutants, both in diploids and tetraploids.

Please note: Wiley is not responsible for the content or functionality of any Supporting Information supplied by the authors. Any queries (other than missing material) should be directed to the *New Phytologist* Central Office.

© 2023 The Authors
New Phytologist © 2023 New Phytologist Foundation

14698137, 0, Downloaded from https://nph.onlinelibrary.wiley.com/doi/10.1111/nph.19366 by LEIBNIZ-INST. OF PLANT GENETICS AND CROP PLANT, Wiley Online Library on [23/11/2023]. See the Terms and Conditions (https://onlinelibrary.wiley.com/terms-and-conditions) on Wiley Online Library for rules of use; OA articles are governed by the applicable Creative Commons License